

Electron-Ion Interaction and the Fermi Surfaces of the Alkali Metals

MARTIN J. G. LEE

James Franck Institute and Department of Physics, University of Chicago, Chicago, Illinois 60637

(Received 8 July 1968)

A method is proposed whereby the partial-wave phase shifts which characterize the scattering of plane waves by the ionic cores in a metallic lattice may be deduced from experimental Fermi-surface data. The method is applied to an analysis of currently available experimental data on the shapes of the Fermi surfaces of the alkali metals. Starting from the full many-body theory of conduction electrons in a metallic lattice, it is shown that the shape of the Fermi surface may be derived from a one-electron-like Schrödinger equation which involves a nonlocal effective potential. The augmented-plane-wave method is applied to solve the nonrelativistic Schrödinger equation for the shapes of the surfaces of constant energy in \mathbf{k} space, in the approximation where the effective potential may be represented by an angular-momentum-dependent potential of muffin-tin form. The partial-wave phase shifts of the muffin-tin potential are adjusted to bring the area distortions of the computed surface into agreement with the experimental data. The phase shifts deduced in this way are shown to be largely independent of the radius of the muffin-tin sphere. It is found that the shapes of the Fermi surfaces of the alkali metals are systematically influenced by the position of each metal in the periodic table. Lithium shows a strong p phase shift, which anticipates the onset of the p resonance in the second row of the periodic table. The phase shifts in sodium are found to converge rapidly in angular momentum, presumably because the p -like component of the ionic potential is largely cancelled by the p -like core states, while the d -like component of the ionic potential is rather weak. Potassium, rubidium, and cesium show increasingly strong d phase shifts, which are associated with the positions of these metals at the heads of the $3d$, $4d$, and $5d$ transition series. Only for potassium are the experimental data sufficiently accurate to show the influence of a small f phase shift. The method of phase-shift analysis has several advantages as a technique by which the radial distortions of the Fermi surface of a metal may be deduced from experimental data on the anisotropy of its extremal cross-sectional area. These include rapid convergence of the series of phase shifts, the use of a model surface generated in a way closely related to a first-principles band-structure calculation, and the possibility of applying the technique both to nearly-free-electron metals and to metals of the transition series. The radial distortions of the Fermi surfaces of the alkali metals are computed, and the results are compared with those of earlier calculations. Finally, it is shown that our results impose criteria which must be satisfied by any effective potential of muffin-tin form that may be proposed to represent the effects of electron exchange and correlation in the alkali metals.

INTRODUCTION

IN recent years, experimental studies have yielded quantitative information about the anisotropies of the Fermi surfaces of the alkali metals. Measurements of the de Haas-van Alphen effect in potassium and rubidium were made by Shoenberg and Stiles.¹ Okumura and Templeton² investigated the de Haas-van Alphen effect in cesium, and Lee³ studied the effect in sodium. In each of these investigations, the anisotropy of the extremal cross-sectional area of the Fermi surface was deduced directly from the experimental data, and an inversion scheme was used to estimate the radial anisotropy of the Fermi surface. Experimental difficulties have so far prevented systematic de Haas-van Alphen studies of lithium, but Donaghy and Stewart⁴ applied the somewhat less accurate technique of positron annihilation to measure the extremal cross-sectional areas of the Fermi surface normal to the $\langle 100 \rangle$, $\langle 110 \rangle$, and $\langle 111 \rangle$ symmetry directions, and used an inversion scheme to deduce the radial distortions of the Fermi surface.

The interpretation of the results of these studies is now well established. The experimental data relate to

the Fermi surfaces of the alkali metals in the bcc crystal structure. The extreme radial distortion of the Fermi surface from the free-electron sphere is found to increase from about 0.1% in sodium to 3.3% in cesium, while the Fermi surface of lithium is somewhat more distorted than that of cesium, as shown in Table I.

In addition to experimental studies, the Fermi surfaces of the alkali metals have been the subject of several theoretical discussions. Ham⁵ combined the quantum method with the Green's function method in a systematic study of the band structures of the alkali metals, and was able to predict the observed trend of Fermi surface anisotropy within the alkali series, al-

TABLE I. Experimental-radial distortions of the Fermi surfaces of the alkali metals as given in the literature.^a

	$10^4(k_{100}-k_0)/k_0$	$10^4(k_{110}-k_0)/k_0$	$10^4(k_{111}-k_0)/k_0$
Li ^b	-100±100	+400±100	-100±100
Na ^c	-7.83±0.40	+9.27±0.50	-1.54±0.10
K ^d	+14.7±0.4	+10.8±0.4	-11.0±0.4
Rb ^e	-23±14	+95±5	-46±10
Cs ^f	-94±10	+331±10	-143±10

^a The radii set out above were deduced by the several authors from the experimental area data (Table III) by using various inversion techniques.

^b Reference 4.

^c Reference 3.

^d Reference 9.

^e Reference 1.

^f Reference 2.

⁵ F. S. Ham, Phys. Rev. **128**, 82 (1962); **128**, 2524 (1962).

¹ D. Shoenberg and P. J. Stiles, Proc. Roy. Soc. (London) **A281**, 62 (1964).

² K. Okumura and I. M. Templeton, Proc. Roy. Soc. (London) **A287**, 89 (1965).

³ M. J. G. Lee, Proc. Roy. Soc. (London) **A295**, 440 (1966).

⁴ J. J. Donaghy and A. T. Stewart, Phys. Rev. **164**, 391 (1967).

though his calculated distortions were rather larger than those found experimentally, and the shapes of the computed Fermi surfaces of potassium, rubidium, and cesium did not agree in detail with the experimental data. Heine and Abarenkov⁶ calculated the band structures of the alkalis from their model potential,⁷ and found that the computed Fermi surfaces were considerably less distorted than those found by Ham, and therefore in rather better agreement with experiment. However, Heine and Abarenkov did not make detailed predictions of the shapes of the Fermi surfaces of the alkali metals. Ashcroft⁸ analyzed the experimental data of Shoenberg and Stiles on potassium and rubidium in terms of a local pseudopotential, and Lee⁹ carried out a similar calculation for the experimental data on sodium. Lee and Falicov⁹ showed that the shape of the Fermi surface of potassium is strongly influenced by low-lying *d*-like energy bands, and that certain features of the experimental data can be explained only if nonlocality (angular momentum dependence) is introduced into the pseudopotential.

There is no reason to believe that potassium is alone in this respect. The low-lying *d*-bands are associated with the position of potassium at the head of the 3*d* transition series in the periodic table. Rubidium and cesium occupy similar positions in relation to the 4*d* and 5*d* transition series, and presumably the distortions of their Fermi surfaces would also be influenced by the low-lying *d*-like energy bands. Similarly, the shape of the Fermi surface of lithium would be influenced by the *p*-like energy band just above the Fermi surface. Finally, the Fermi surface of sodium might be expected to show some residual nonlocal effects, although nonlocal effects are known to be weak in the second row series Na,³ Mg,¹⁰ and Al,¹¹ because of the partial cancellation of the *s*- and *p*-like components of the ionic potential by the *s*- and *p*-like core states.

The aim of the present paper is to interpret the experimental data on the shapes of the Fermi surfaces of the alkali metals in terms of the interaction between the conduction electrons and the ionic lattice. We have found it convenient to represent the nonlocal effects directly in terms of the partial-wave phase shifts which describe the scattering of plane waves by the ionic potential. We begin by describing the calculational scheme; then the analysis of the experimental data is set out, and finally the results and conclusions of this work are discussed.

⁶ V. Heine and I. Abarenkov, *Phil. Mag.* **9**, 451 (1964).

⁷ I. Abarenkov and V. Heine, *Phil. Mag.* **12**, 529 (1965).

⁸ N. W. Ashcroft, *Phys. Rev.* **140**, 935 (1965).

⁹ M. J. G. Lee and L. M. Falicov, *Proc. Roy. Soc. (London)* **A304**, 319 (1968).

¹⁰ J. C. Kimball, R. W. Stark, and F. M. Mueller, *Phys. Rev.* **162**, 600 (1967).

¹¹ N. W. Ashcroft, *Phil. Mag.* **8**, 2055 (1963).

METHOD OF CALCULATION

Schrödinger Equation

The one-particle Green function¹² for a system of nonrelativistic interacting electrons in thermal equilibrium with an ionic lattice may be expressed in the operator form

$$G(\mathbf{r}, \mathbf{p}, E) = [E - (p^2/2m) - V_0(\mathbf{r}) - \Sigma(\mathbf{r}, \mathbf{p}, E)]^{-1}, \quad (1)$$

where E is the complex generalization of the single-particle energy of a system of noninteracting particles, $V_0(\mathbf{r})$ consists of the bare nuclear potential together with the Hartree field of the electrons, and $\Sigma(\mathbf{r}, \mathbf{p}, E)$ is a complex operator (the proper self-energy) which includes all exchange, correlation, and lifetime effects.

The poles of $G(\mathbf{r}, \mathbf{p}, E)$ determine the energies of those elementary excitations of the system which correspond to the single-particle excitations of a system of noninteracting particles. The complex energies of these elementary excitations, the Landau quasiparticles, are therefore solutions of the Dyson equation which, expressed as a relation between operators, takes the form

$$(p^2/2m) + V_0(\mathbf{r}) + \Sigma(\mathbf{r}, \mathbf{p}, E) = E. \quad (2)$$

The imaginary part of Σ vanishes at the Fermi level of a metal in the limit of zero temperature. In many band-structure problems, and especially those involving the Fermi surface, it is an adequate approximation to consider only the real part of Σ . Then the Dyson equation reduces to a single-particle-like Schrödinger equation

$$\mathcal{H}(E)\phi(\mathbf{r}, E) = E\phi(\mathbf{r}, E), \quad (3)$$

where

$$\mathcal{H}(E) = (p^2/2m) + V_0(\mathbf{r}) + \text{Re}\Sigma(\mathbf{r}, \mathbf{p}, E). \quad (4)$$

In a crystal lattice, the structural periodicity of $\mathcal{H}(E)$ leads at once to a Schrödinger equation of the form

$$\mathcal{H}(E_n(\mathbf{k}))\phi_{n,\mathbf{k}}(\mathbf{r}) = E_n(\mathbf{k})\phi_{n,\mathbf{k}}(\mathbf{r}), \quad (5)$$

where the parametric energy dependence of the wave function has been absorbed into the band index. Thus it follows from the Dyson equation of many-body theory that, under the assumption that lifetime effects are negligible, the band structure is the set of eigenvalues of the one-electron-like Schrödinger equation

$$[-(\hbar^2/2m)\nabla^2 + V_{\text{eff}}(\mathbf{r}, \mathbf{p}, E)]\phi_{n,\mathbf{k}}(\mathbf{r}) = E_n(\mathbf{k})\phi_{n,\mathbf{k}}(\mathbf{r}), \quad (6)$$

where $V_{\text{eff}}(\mathbf{r}, \mathbf{p}, E)$ is a nonlocal effective potential defined by

$$V_{\text{eff}}(\mathbf{r}, \mathbf{p}, E) = V_0(\mathbf{r}) + \text{Re}\Sigma(\mathbf{r}, \mathbf{p}, E). \quad (7)$$

That exchange and correlation corrections may be folded into an energy- and momentum-dependent effective potential accounts for the well-known success of the one-electron picture as a description of the dynamics

¹² See, e.g., D. A. Kirzhnits, *Field Theoretical Methods in Many-Body Systems* (Pergamon Press, Inc., Oxford, 1967); V. Heine, P. Nozieres, and J. W. Wilkins, *Phil. Mag.* **13**, 741 (1966).

of conduction electrons in normal metals. Similarly we may expect to obtain good agreement with the experimental Fermi surface distortions by solving the one-electron Schrödinger equation self-consistently in the metallic lattice, treating the effective potential as a function to be determined from the experimental data.

As a first step towards solving the Schrödinger equation (6) it is helpful to transform the momentum dependence of the effective potential so that dependence on the radial and transverse components of momentum may be treated separately. We assume that the radial contribution can be absorbed into the energy dependence of the effective potential, and that the transverse contribution can be expressed as an angular momentum dependence of the effective potential. In this approximation the Schrödinger equation takes the form

$$[-(\hbar^2/2m)\nabla^2 + V_{\text{eff}}(\mathbf{r}, l, E)]\phi_{n, \mathbf{k}}(\mathbf{r}) = E_n(\mathbf{k})\phi_{n, \mathbf{k}}(\mathbf{r}). \quad (8)$$

The work of Bohm and Pines¹³ has demonstrated that, in a free-electron gas, correlation effects tend to cancel the rather strong momentum dependence of the Hartree-Fock exchange potential. Since the residual momentum dependence of the effective potential is weak, we would expect the approximation leading to Eq. (8) to work well, especially for Fermi surface calculations.

Secular Determinant

Of the many techniques that have been developed to solve the one-electron Schrödinger equation (8) in an infinite crystalline lattice, we have selected Slater's method of augmented plane waves.¹⁴ The APW method shares with the Green's function (KKR) method of Korringa¹⁵ and Kohn and Rostoker¹⁶ the advantage that the one-electron potential may be introduced into the calculations as a set of partial-wave phase

shifts for the scattering of plane waves by the ion cores. It was anticipated that changes of the computed Fermi surface distortions would be substantially linear for small variations of the phase shifts, and that for the alkali metals only the first two or three phase shifts would differ significantly from zero. These properties were amply confirmed in the course of the present work, and they combine to simplify the analysis of experimental data. In general the KKR method might be more convenient as a calculational scheme than the APW method since it involves a smaller secular determinant and can be programmed in a way more economical of computer time. The structure factors of the Green's function method have, however, a singularity on the free-electron Fermi sphere,¹⁷ and since this might well introduce errors into calculations of the Fermi surfaces of the more free-electron-like of the alkali metals, the APW method was preferred.

In its simplest form, the form we shall use here, the APW method may be applied to determine the energy bands and wave functions in a crystalline solid in which the potential is radially symmetric within non-intersecting spheres centered on each lattice site, and constant elsewhere. Such a potential is said to be of muffin-tin form. It is convenient to set the constant potential between the muffin-tin spheres equal to zero; this defines the APW scale of energy.

The APW method has been described many times, and for a derivation and discussion of the secular determinant the reader is referred to the literature.¹⁸ A variational argument shows that the relation between energy E and wave vector \mathbf{k} for conduction electrons in a crystalline lattice is the solution of a secular equation of the form¹⁹

$$\det\{[(\mathbf{k} + \mathbf{g})^2 - E]\delta_{\mathbf{g}\mathbf{g}'} + \Gamma_{\mathbf{g}\mathbf{g}'}(\mathbf{k}, E)\} = 0, \quad (9)$$

where, for a crystal with one atom per primitive cell

$$\Gamma_{\mathbf{g}\mathbf{g}'}(\mathbf{k}, E) = (4\pi R_S^2/\Omega) \left\{ -[(\mathbf{k} + \mathbf{g}') \cdot (\mathbf{k} + \mathbf{g}) - E] \frac{j_1(|\mathbf{g} - \mathbf{g}'| R_S)}{|\mathbf{g} - \mathbf{g}'|} + \sum_{l=0}^{\infty} (2l+1) P_l(\cos\theta_{\mathbf{g}\mathbf{g}'}) \times j_l(|\mathbf{k} + \mathbf{g}| R_S) j_l(|\mathbf{k} + \mathbf{g}'| R_S) [\mathcal{R}_l'(R_S, E)/\mathcal{R}_l(R_S, E)] \right\}. \quad (10)$$

In this equation, \mathbf{g} and \mathbf{g}' are the reciprocal lattice vectors of the crystal structure, R_S is the radius of the spherical part of the muffin-tin potential, Ω is the atomic volume, $\theta_{\mathbf{g}\mathbf{g}'}$ is the angle between the reciprocal lattice vectors \mathbf{g} and \mathbf{g}' , and $[\mathcal{R}_l'(R_S, E)/\mathcal{R}_l(R_S, E)]$ is the logarithmic derivative of the solution of the radial

¹³ D. Bohm and D. Pines, Phys. Rev. **92**, 609 (1953); D. Pines, *ibid.* **92**, 626 (1953).

¹⁴ J. C. Slater, Phys. Rev. **51**, 846 (1937); **92**, 603 (1953).

¹⁵ J. Korringa, Physica **13**, 392 (1947).

¹⁶ W. Kohn and N. Rostoker, Phys. Rev. **94**, 1111 (1954); F. S. Ham and B. Segall, *ibid.* **124**, 1786 (1961).

¹⁷ K. H. Johnson, Phys. Rev. **150**, 429 (1966).

¹⁸ For an introduction to many of the practical aspects of the APW method, and for a guide to the literature, see T. Loucks, *The Augmented Plane Wave Method* (W. A. Benjamin, Inc., New York, 1967).

¹⁹ Note that all quantities in Eqs. (9)–(11) are expressed in atomic units. The unit of energy is the rydberg, and the unit of length is the Bohr radius.

TABLE II. Numerical values of various parameters of the alkali metals that are needed in the present calculations.

	a_0^a (a. u.)	R_I^b (a. u.)	E_F^{0c} (Ry)	$E_F^{1d,e}$ (Ry)	$E_F^{2f,g}$ (Ry)	$E_F^{3g,h}$ (Ry)
Li	6.597	2.856	0.3491	0.2442		
Na	7.984	3.457	0.2384	0.2118		
K	9.873	4.275	0.1559		0.1424	
Rb	10.554	4.570	0.1364	0.1361	0.1292	
Cs	11.424	4.947	0.1165	0.1156	0.1081	0.1737

^a a_0 is the lattice constant.
^b R_I is the inscribed-sphere radius.
^c E_F^0 is the free-electron Fermi energy.
^d E_F^1 is the Fermi energy from APW calculations—Slater exchange.
^e J. F. Kenney (private communication).
^f E_F^2 is the Fermi energy from self-consistent APW calculations—Slater exchange.
^g E_F^3 is the Fermi energy from self-consistent APW calculations—Kohn and Sham exchange.

Schrödinger equation

$$-\frac{1}{r^2} \frac{\partial}{\partial r} \left(r^2 \frac{\partial \mathcal{R}_l(r)}{\partial r} \right) + \left[\frac{l(l+1)}{r^2} + V_{\text{eff}}(r, l, E) \right] \mathcal{R}_l(r) = E \mathcal{R}_l(r), \quad (11)$$

calculated at the muffin-tin radius R_S .²⁰

Since the muffin-tin potential is of finite range, the logarithmic derivatives of the radial wave function may be related to the partial-wave-scattering phase shifts $\eta_l(E)$ of the effective potential by the equation²¹

$$\frac{\mathcal{R}_l'(R_S, E)}{\mathcal{R}_l(R_S, E)} = \left[\frac{j_l'(kr) - \tan \eta_l(E) y_l'(kr)}{j_l(kr) - \tan \eta_l(E) y_l(kr)} \right]_{r=R_S}, \quad (12)$$

where $k^2 = E$. The effective potential enters into the secular determinant (9) only to the extent that it determines the logarithmic derivatives of the radial wave function. On substituting (12) into (9), it will be seen that the shape of the surface of constant energy E is fully determined by the set of phase shifts $\eta_l(E)$.

Digital computer programs were developed to calculate from Eqs. (9), (10), and (12), the radii and the

TABLE III. Experimental-area distortions of the Fermi surfaces of the alkali metals.

	$10^4(A_{100}-A_0)/A_0$	$10^4(A_{110}-A_0)/A_0$	$10^4(A_{111}-A_0)/A_0$
Li ^a	-110±85	-310±85	+140±85
Na ^b	-2.04±0.20	-2.00±0.20	+7.15±0.40
K ^c	+14.15±0.44	-4.65±0.22	+2.36±0.12
Rb ^d	+38.4±2.2	-27.9±2.2	+56.5±2.2
Cs ^e	+110±10	-87±10	+214±10

^a Reference 4.
^b Reference 3.

^c Reference 9.
^d Reference 1.

^e Reference 2.

²⁰ The most rapid convergence results if the muffin-tin radius R_S is set equal to the inscribed-sphere radius R_I . For the present calculations we have taken $R_S = R_I = (\sqrt{3}/4)a_0$, where a_0 is the lattice parameter of the structure.

²¹ A. Messiah, *Quantum Mechanics* (North-Holland Publishing Co., Amsterdam, 1961), p. 390. For the spherical Bessel functions we have adopted the notation and definitions of M. Abramowitz and I. A. Stegun, *Handbook of Mathematical Functions* (Dover Publications, Inc., New York, 1965).

cross-sectional areas of the surfaces of constant energy for a given energy E and a given set of phase shifts $\eta_l(E)$. The radius of the surface of constant energy in a given direction was determined by computing the secular determinant (9) for a series of wave vectors of increasing magnitude in that direction. An inverse interpolation technique was then applied to determine the magnitude of the wave vector for which the determinant vanished, and which would therefore lie on the surface of constant energy E . In the areas program, the extremal cross-sectional areas of the surfaces of constant energy were found by numerical integration of the radii. Checks of convergence showed that the accuracy of the interpolation and integration techniques was such that they introduced no appreciable error into subsequent calculations.

In each program the phase shifts $\eta_l(E)$ for $l=0, 1$, and 2 were treated as adjustable parameters. The phase shifts $\eta_l(E)$ for $l=3$ through 12 were set equal to zero, and the summation was truncated beyond $l=12$. Convergence checks showed that truncation of the sum over l introduces no appreciable error into the calculations; our neglect of higher phase shifts is a significant approximation and will be discussed below.

The calculations were carried out with a 30×30 secular determinant. Convergence was found to be excellent, despite the relatively small secular determinant; doubling the size of the secular determinant caused no perceptible change in the shapes of the computed surfaces. A more detailed discussion of convergence will be postponed until the results of the calculations have been presented.

Scattering Phase Shifts

When the effective potential in Eq. (8) is zero, the solutions of the radial Schrödinger equation (11) are spherical Bessel functions of the first kind, whose logarithmic derivatives are

$$\mathcal{R}_l'(R_S, E) / \mathcal{R}_l(R_S, E) = j_l'(kR_S) / j_l(kR_S). \quad (13)$$

The phase shifts corresponding to a zero potential within the muffin-tin sphere are, from (12) and (13), zero. Thus the free-electron band structure, and hence spherical surfaces of constant energy, are generated if the phase shifts in the APW secular determinant are set equal to zero. A weak attractive potential increases the phase shifts from zero in a positive sense, and as each bound state is drawn into the potential well the phase shift corresponding to the angular momentum character of the bound state increases rapidly by π . Only the tangents of the phase shifts enter into the secular determinant, however, and the distortions from sphericity of the surfaces of constant energy are determined by the "reduced" phase shifts, from which all integral multiples of π have been subtracted.

In order to calculate the shape of the Fermi surface, the energy parameter E in the secular equation (9)

TABLE IV. Partial-wave phase shifts for the alkali metals as deduced in the course of the present work.

	E_F^a	η_0^b	η_1^b	η_2^b	$\mathfrak{F}(E)^c$
Li	0.24	+0.0633±0.3200	+0.1834±0.0154	-0.0102±0.0248	+0.3582
	0.28	-0.0653±0.3200	+0.1604±0.0154	-0.0165±0.0248	+0.2120
	0.32	-0.1887±0.3200	+0.1280±0.0154	-0.0244±0.0248	+0.0465
	0.36	-0.2883±0.3200	+0.0876±0.0154	-0.0354±0.0248	-0.1289
Na	0.20	+0.3128±0.0092	+0.0205±0.0016	-0.0002±0.0008	+0.2376
	0.21	+0.2587±0.0092	+0.0080±0.0016	-0.0013±0.0008	+0.1758
	0.22	+0.2034±0.0092	-0.0047±0.0016	-0.0023±0.0008	+0.1130
	0.23	+0.1481±0.0092	-0.0179±0.0016	-0.0034±0.0008	+0.0493
K	0.14	-0.0136±0.0022	+0.0337±0.0002	+0.0247±0.0003	+0.1343
	0.15	-0.0769±0.0022	+0.0123±0.0002	+0.0244±0.0003	+0.0521
	0.16	-0.1381±0.0022	-0.0109±0.0002	+0.0233±0.0003	-0.0346
	0.17	-0.1977±0.0022	-0.0351±0.0002	+0.0216±0.0003	-0.1241
	0.18	-0.2577±0.0022	-0.0607±0.0002	+0.0194±0.0003	-0.2184
	0.19	-0.3177±0.0022	-0.0863±0.0002	+0.0172±0.0003	-0.3127
Rb	0.12	+0.0402±0.0115	+0.0135±0.0017	+0.0321±0.0014	+0.1534
	0.13	-0.0372±0.0115	-0.0108±0.0017	+0.0334±0.0014	+0.0621
	0.14	-0.1048±0.0115	-0.0384±0.0017	+0.0333±0.0014	-0.0341
	0.15	-0.1706±0.0115	-0.0678±0.0017	+0.0321±0.0014	-0.1358
Cs	0.09	+0.1363±0.0312	+0.0197±0.0054	+0.0401±0.0036	+0.2522
	0.10	+0.0460±0.0312	-0.0068±0.0054	+0.0450±0.0036	+0.1594
	0.11	-0.0462±0.0312	-0.0353±0.0054	+0.0499±0.0036	+0.0618
	0.17	-0.5131±0.0312	-0.2485±0.0054	+0.0462±0.0036	-0.6542

^a E_F is assumed Fermi energy on the APW scale (Ry).

^b η_0, η_1, η_2 are phase shifts in radians; higher phase shifts are set equal to zero.

^c $\mathfrak{F}(E)$ is the Friedel sum of the phase shifts as defined in Eq. (14).

must be set equal to the Fermi energy measured on the APW scale (E_F). Since this quantity is not known, our calculations were carried out for a series of energies close to the free-electron Fermi energy. The range of energies was guided by the results of first-principles APW calculations, as set out in Table II. At each energy, the phase shifts $\eta_0, \eta_1,$ and η_2 were adjusted to bring the radial distortions of the computed Fermi surface from the free-electron sphere into agreement with the experimental radial distortions of the Fermi surface along the symmetry directions, as quoted in Table I. Slight adjustments of the phase shifts were then made to bring the area distortions of the computed Fermi surface from the free-electron sphere into agreement with the area distortions of the Fermi surface normal to the symmetry directions as quoted in Table III, since these are the primary experimental quantities. The remarkable linearity of the computed Fermi surface distortions for small changes of the phase shifts at fixed energy contributed to the rapid convergence of these adjustments. It should perhaps be emphasized that as all distortions are measured with respect to the free-electron Fermi sphere, the Fermi surfaces computed in this way necessarily have a volume, within the accuracy of the calculation, of one electron per atom. In particular, knowledge of the volume of the Fermi surface offers no guide to the correct choice of the Fermi energy parameter E_F . However, the phase shifts corresponding to a particular choice of E_F are uniquely defined by this procedure.

RESULTS

In Table IV we present the final results of the phase-shift calculations. The reduced phase shifts $\eta_0, \eta_1,$ and

η_2 for the five alkali metals are given for a series of values of the Fermi energy parameter E_F . The probable errors in the phase shifts were computed from the experimental errors in the area distortions. Also given in Table IV are the Friedel sums of the phase shifts, which are defined by²²

$$\mathfrak{F}(E) = \mathfrak{F}[\eta_l(E)] = - \sum_{l=0}^{\infty} (2l+1) \eta_l(E). \quad (14)$$

In subsequent discussion we shall refer to the phase shifts for $l=0, l=1, l=2,$ and $l=3$ as the $s, p, d,$ and f phase shifts, respectively.

Fermi Energy Parameter

That a fundamental relation exists between the assumed Fermi energy E_F and the corresponding set of phase shifts $\eta_l(E_F)$ may be seen by considering the change in occupied electronic states as the reduced phase shifts η_l are taken from zero, corresponding to the free-electron model with Fermi energy E_F^0 , to their final values $\eta_l(E_F)$. An elementary argument²³ shows that for a solid of N atoms, a total of $N\mathfrak{F}(E_F)$ electronic states are displaced into the surface in \mathbf{k} space for which $|\mathbf{k}|^2 = E_F$. Since by hypothesis E_F is the Fermi energy corresponding to the final set of phase shifts $\eta_l(E_F)$, the displaced electronic states must be just sufficient in number to hold those electrons whose energies on the free-electron model were greater than E_F . If the surfaces of constant energy are assumed to remain spherical, the relation between the assumed

²² J. Friedel, *Advan. Phys.* 3, 446 (1954); note that the phase shifts are expressed in radians.

²³ C. Kittel, *Quantum Theory of Solids* (John Wiley & Sons, Inc., New York, 1963), p. 341.

TABLE V. Sensitivity of the shape of the computed Fermi surface to the value assumed for E_F .^a

	$10^4(k_{100}-k_{111})/k_0$	$10^4(k_{110}-k_{111})/k_0$
Li	$-80.0 \pm 150.0 (\pm 3.0)$	$722.0 \pm 150.0 (\pm 7.0)$
Na	$-7.1 \pm 0.4 (\pm 0.1)$	$10.3 \pm 0.5 (\pm 0.1)$
K	$25.7 \pm 0.6 (\pm 0.6)$	$25.0 \pm 0.6 (\pm 0.5)$
Rb	$42.2 \pm 17.0 (\pm 2.1)$	$154.6 \pm 11.0 (\pm 1.2)$
Cs	$87.0 \pm 15.0 (\pm 1.9)$	$529.0 \pm 15.0 (\pm 5.0)$

^a The radial distortions given above are those deduced in the course of the present work. The errors represent the uncertainty in the radial distortions due to experimental error. The errors in parentheses indicate the variation of the radial distortions deduced from the best fit of the area data with the range of values of E_F shown in Table IV.

Fermi energy and the Friedel sum of the phase shifts takes the form

$$[1 - (E_F/E_F^0)^{3/2}] = \mathfrak{F}(E_F). \quad (15)$$

For small displacements of energy from the free-electron Fermi energy, this equation reduces to the linear form

$$(E_F^0 - E_F)/E_F^0 \approx \frac{2}{3} \mathfrak{F}(E_F). \quad (16)$$

Although this simple relation holds quantitatively only for spherical surfaces of constant energy, there exists even for highly distorted surfaces a unique relation between the assumed Fermi energy measured on the APW scale and the Friedel sum of the corresponding set of phase shifts. The existence of such a relation was very helpful in guiding and checking the calculations leading to the results set out in Table IV.

The physical requirement that the charge distribution of the conduction electrons should be consistent with an assumed ionic potential would allow one to determine the correct value of E_F . However, current first principles calculations offer no clear guide to the correct value of E_F , since it turns out that the computed value of E_F is very sensitive to the way exchange and correlation effects are taken into account (Table II), and the most appropriate potential remains a subject

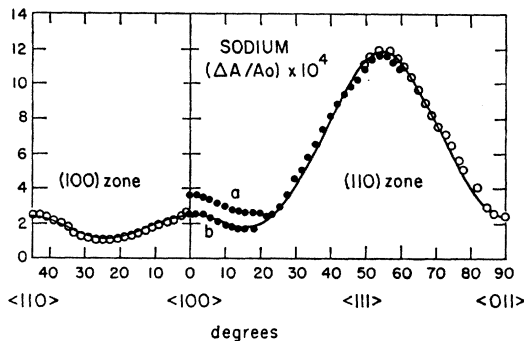


FIG. 1. The computed area distortions of the Fermi surface of sodium together with typical experimental data in the (100) and (110) symmetry zones (Ref. 24). The surface was computed with the set of phase shifts corresponding to $E_F = 0.22$ Ry. The area distortions are calculated with respect to an arbitrary sphere somewhat smaller than the free-electron Fermi sphere. The extremal cross section of the free-electron Fermi sphere corresponds to the ordinate $(\Delta A/A_0) \times 10^4 \approx 4.7$.

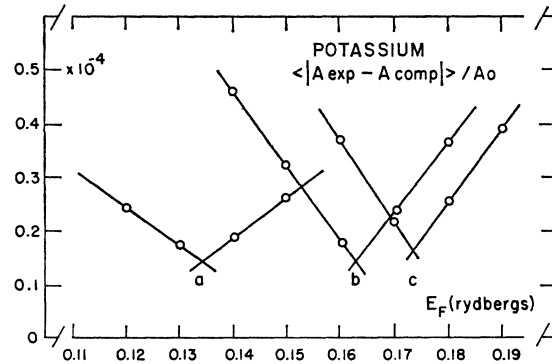


FIG. 2. The mean deviation of the computed area distortions of the Fermi surface of potassium from the experimental data, as a function of E_F , for three different values of the j phase shift. The results suggest that apparent sensitivity to the choice of E_F of the fit to the experimental data may reflect incomplete convergence of the series of phase shifts (Ref. 25).

of discussion. An experimental method of determining E_F is suggested by a physical interpretation of the Friedel sum of the phase shifts. An extension of the arguments above²³ shows that the fraction of conduction charge that is displaced into the region of the muffin-tin spheres by the ionic potential is equal to the Friedel sum of the phase shifts, and hence the Fermi energy, could be computed if one knew the distribution of conduction charge density in the metal. However, no x-ray measurements have so far been made of sufficient accuracy to allow one to deduce the distribution of conduction charge in the alkali metals.

In the absence of reliable information about the correct choice of E_F , we prefer to regard E_F as a further parameter in the fit to the Fermi-surface data, and we now investigate the influence of this parameter. The anisotropy of the extremal cross-sectional area of the Fermi surface of sodium as computed from the set of phase shifts corresponding to $E_F = 0.22$ Ry (Table IV) is illustrated in Fig. 1.²⁴ It will be seen that the area distortions of the computed Fermi surface are in good agreement with the experimental data. That this agreement does not depend significantly on the choice of the energy parameter E_F is demonstrated in Table V, where the sensitivities of the radii of the computed Fermi surfaces of the alkali metals to variations in the value of E_F are compared with the uncertainties in the radii implied by the errors in the experimental data.

²⁴ The experimental data are taken from Ref. 3. Data in the (100) zone are from sample 16, while data in the (110) zone are from sample 11(2) (full circles), and from sample 3 (open circles). Curves (a) and (b) represent two possible interpretations of the experimental data from sample 11(2); (a) is the interpretation of the data given in Ref. 3, while (b), which differs from (a) by the arbitrary addition of π rad to the experimental de Haas-van Alphen phase, is more generally consistent with the experimental data in the (100) zone. The possibility of missing a phase change of π in regions of small signal amplitude is discussed in Ref. 3. However, the reinterpretation of the experimental data as in (b) must be regarded as tentative.

The results in Table V show that, for potassium alone among the alkali metals, the computed Fermi surface is sensitive to changes in E_F to an extent comparable with the accuracy of the experimental data. A more detailed analysis of the experimental data for potassium was therefore undertaken. The area distortions of the Fermi surface were computed at 10° intervals in the $[100]$ and $[110]$ zones for each of the sets of phase shifts and energies in Table IV. The mean deviation of the area distortions from the experimental data of Lee⁹ was then computed, and is plotted as a function of E_F in Fig. 2. The best fit to the experimental data was found with $E_F \approx 0.162 \pm 0.005$ Ry.

So far we have discussed the analysis of the Fermi-surface data in terms of the s , p , and d phase shifts, and have set the f and higher phase shifts equal to zero. In order to consider the possible influence of the f phase shift on our determination of the best value of E_F for potassium, the computer program was modified to allow for nonzero values of η_3 . The f phase shift was set equal to $+0.0005$ rad and to -0.0005 rad, and the s , p , and d phase shifts were again adjusted to fit the experimental area distortions normal to the symmetry directions. The mean deviation of the computed surface from the experimental data was again calculated for several values of E_F , and the best fit to the experimental data (Fig. 2) was found with

$$E_F = (0.134 \pm 0.005) \text{ Ry}, \quad \eta_3 = +0.0005 \text{ rad},$$

$$E_F = (0.173 \pm 0.005) \text{ Ry}, \quad \eta_3 = -0.0005 \text{ rad}.$$

Thus the apparent sensitivity of the computed surface to small changes in the energy parameter E_F suggests a small but significant influence of the f phase shift on the shape of the Fermi surface of potassium.

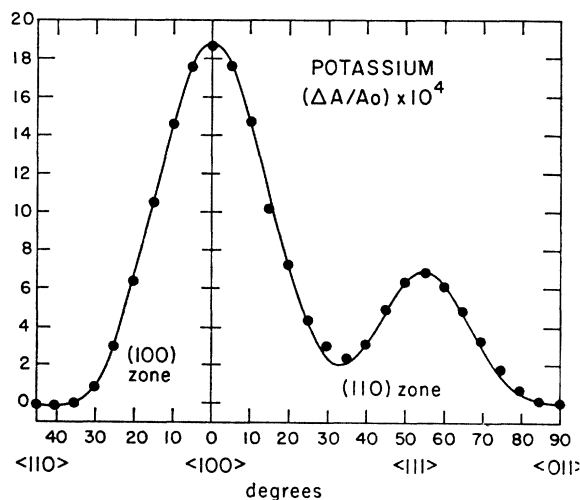


FIG. 3. The computed area distortions of the Fermi surface of potassium, together with mean experimental data in the (100) and (110) symmetry zones (Ref. 28). The surface was computed with the set of phase shifts corresponding to $E_F = 0.16$ Ry. The extremal cross section of the free-electron Fermi sphere corresponds to the ordinate $(\Delta A/A_0) \times 10^4 \approx 4.6$.

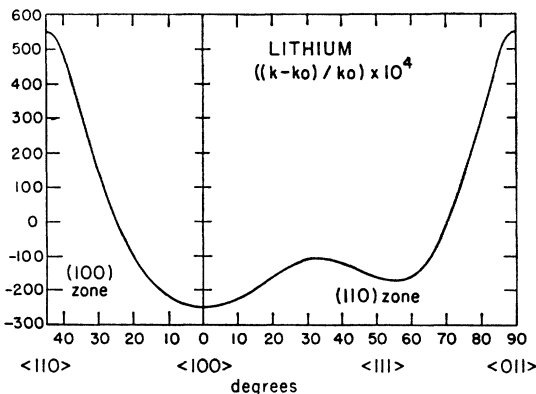


FIG. 4. The computed radial distortions of the Fermi surface of lithium, derived from the set of phase shifts corresponding to $E_F = 0.28$ Ry.

For this reason, the value of E_F cannot be estimated from the experimental data independently of some assumption about the magnitude of the f phase shift. Since there are no f -like core states in potassium, we expect the f phase shift to be positive, however, and our results suggest an upper bound on E_F :

$$E_F \leq (0.162 \pm 0.005) \text{ Ry}.$$

In Fig. 3 we compare the area distortions of the computed Fermi surface of potassium with the experimental data. The mean deviation of the fractional area distortions of the computed surface from the experimental data (Fig. 2) is little greater than the estimated experimental error in the data.²⁵

Fermi-Surface Distortions

Our success in fitting the experimental Fermi-surface data for potassium to high accuracy with only four adjustable phase shifts and an arbitrary energy pa-

TABLE VI. Comparison of the radial distortions of the Fermi surfaces of the alkali metals taken from the literature with the values deduced in the course of the present work.

	$10^4(k_{100}-k_{111})/k_0$			$10^4(k_{110}-k_{111})/k_0$		
	Previous work	Present work	Experimental error	Previous work	Present work	Experimental error
Li ^a	-4.0	-80.0	± 150.0	500.0	722.0	± 150.0
Na ^b	-6.3	-7.1	± 0.4	10.8	10.3	± 0.5
K ^c	25.7	25.7	± 0.6	21.8	25.0	± 0.6
Rb ^d	23.0	42.2	± 17.0	141.0	154.6	± 11.0
Cs ^e	49.0	87.0	± 15.0	474.0	529.0	± 15.0

^a Reference 4.

^b Reference 3.

^c Reference 9.

^d Reference 1.

^e Reference 2.

²⁵ The mean deviation of the best fit to the experimental data is about $\pm(0.15 \times 10^{-4})$, while the random error in the data is estimated as $\pm(0.05 \times 10^{-4})$. The difference between these figures reflects a small systematic deviation of the area distortions of the computed surface from the experimental data. It will be seen (Fig. 3) that the systematic deviation is largely confined to the (110) zone, and that more experimental data in this zone would be needed to decide whether or not the discrepancy is significant.

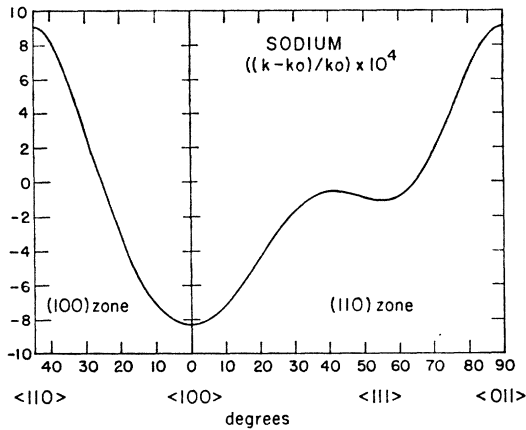


FIG. 5. The computed radial distortions of the Fermi surface of sodium, derived from the set of phase shifts corresponding to $E_F = 0.22$ Ry.

parameter suggests that the method of phase-shift analysis may provide a reliable scheme for fitting the experimental data on the other alkali metals and for estimating the radial distortions of their Fermi surfaces from the experimental area distortions. For these other alkali metals, the sensitivity of the shape of the computed Fermi surface to variations in the energy parameter is substantially less than the uncertainty in the experimental data (Table V). Therefore the experimental data are not sufficiently accurate to allow one to detect the influence of the f and higher phase shifts. In particular, the very small sensitivity of the shape of the computed Fermi surface of sodium to variations in E_F suggests that the f phase shift in that metal may be very small.

The distortions of the radii and of the extremal cross-sectional areas of the Fermi surfaces of the alkali metals were computed from the set of phase shifts corresponding to a Fermi energy parameter E_F close to the free-electron Fermi energy E_F^0 . We have seen that potassium is the only metal for which agreement with the experimental data is sensitive to the choice of E_F ; for potassium we have set E_F equal to the value which gives the best over-all agreement with the data. The radial distortions of the Fermi surfaces of the alkali metals deduced in this way are illustrated in Figs. 4–8, and our best assessment of the distortions between symmetry directions is set out in Table VI. It will be seen that there are some significant discrepancies between our computed radial distortions and those quoted from the literature. The method of phase-shift analysis is closely related to a first-principles band-structure calculation, so the model surfaces constructed by the phase-shift method should be substantially more accurate than those constructed by the various methods that have been used in the past. Furthermore, the phase-shift method involves only the cross-sectional areas of the Fermi surfaces normal to the $\langle 100 \rangle$, $\langle 110 \rangle$, and $\langle 111 \rangle$ symmetry directions, in which directions the data is least sensitive to experimental errors. For these

reasons we believe that our results quoted in Table VI represent the more reliable assessment of the radial distortions of the Fermi surfaces of the alkali metals.

Accuracy of the Calculations

Our calculation of the partial-wave phase shifts from the experimental Fermi-surface distortions in the way discussed above involves several approximations and possible sources of error. Careful tests of convergence have shown that the errors introduced by truncating the sum in the secular determinant (10) beyond $l=12$ were several orders of magnitude smaller than the errors in the experimental data. Similarly, the interpolation technique for locating the zeroes of the secular determinant, and the integration technique developed to compute the area distortions of the surfaces of constant energy, were found to introduce no appreciable errors into the calculation. The areas of the computed surfaces of constant energy in a plane normal to a given direction were found by numerical integration of the radii calculated at a fixed angular interval of rotation in that plane. The integration formula was

$$\delta A = \left[\frac{1}{2} (r_1^2 + r_2^2) \right] \frac{1}{2} (\delta\theta),$$

where δA is the area of a sector bounded by radii r_1 and r_2 , and $\delta\theta$ is the vertex angle of the sector. In the course of the area calculations the basic angular interval was between 5° and 9° , and convergence was checked by doubling this interval and recalculating the area. It was found that the corresponding change in the computed area was about 1 in 10^6 for the sodium and potassium calculations, 1 in 10^5 for the rubidium, 1 in 2000 for the lithium and cesium calculations. Comparison of these results with the experimental data in Table III shows that the integration procedure does not introduce significant errors in the interpretation of the experimental data.

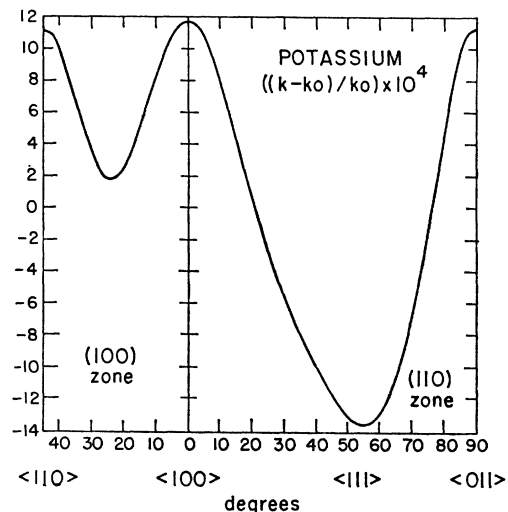


FIG. 6. The computed radial distortions of the Fermi surface of potassium, derived from the set of phase shifts corresponding to $E_F = 0.16$ Ry.

Among the other approximations in the calculation, the only ones that might lead to errors in the final results of the same order as those contributed by the experimental error are the truncation of the secular determinant, the truncation of the series of phase shifts, and the use of a secular determinant based on a muffin-tin potential. These approximations deserve further discussion.

The secular determinant was truncated beyond 30 reciprocal lattice vectors. APW's were included in the basis set corresponding to all reciprocal lattice vectors \mathbf{g} for which

$$|\mathbf{k} + \mathbf{g}| \leq 5.0(\pi/a), \quad (17)$$

where \mathbf{k} is a wave vector on the free-electron sphere at the center of the $1/48$ sector of the Brillouin zone within which the calculations were carried out. The convergence of the final results was checked by increasing the size of the secular determinant to include 40, 50, and finally 60 reciprocal lattice vectors. The results are set out in Table VII. It will be seen that the shape of the computed surface for potassium does not change significantly when the size of the secular determinant is doubled. However, the inclusion of higher matrix elements results in a slight, almost isotropic, contraction of the surfaces of constant energy, and small corrections to the phase shifts are needed to compensate for this effect. Since these corrections (Table VII) are substantially smaller than the errors in the phase shifts which result from experimental error in the data, we conclude that the convergence of the calculations based on the 30×30 secular determinant is satisfactory. This rapid convergence reflects the nearly-free-electron nature of the energy bands at the Fermi energy in the alkali metals. A single APW is needed to reproduce the free-electron energy bands when the reduced phase shifts are set equal to zero. For nonzero phase shifts, the eigenvectors of the secular determinant are linear combinations of APW's constructed in such a way as to eliminate the discontinuity in the derivative of the single APW at the surface of the muffin-tin sphere. In

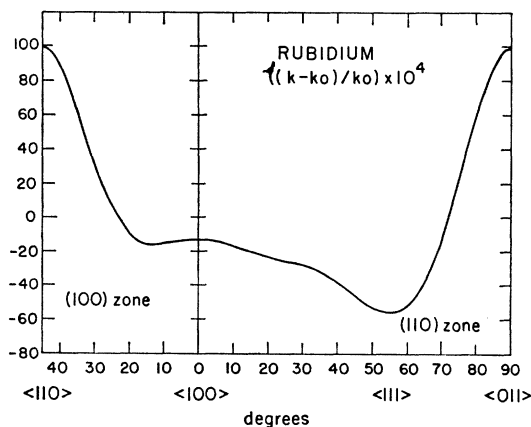


FIG. 7. The computed radial distortions of the Fermi surface of rubidium, derived from the set of phase shifts corresponding to $E_F = 0.14$ Ry.

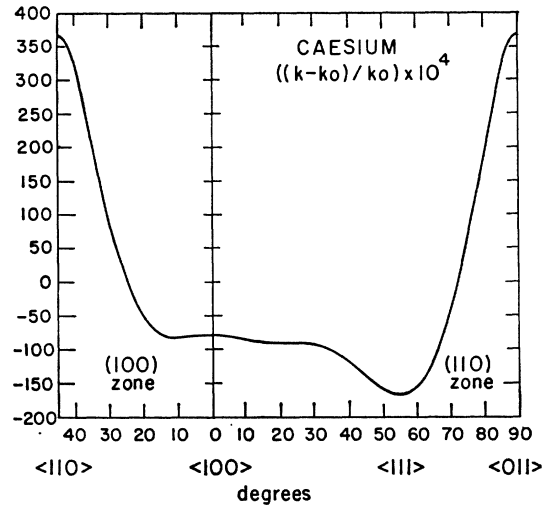


FIG. 8. The computed radial distortions of the Fermi surface of cesium, derived from the set of phase shifts corresponding to $E_F = 0.11$ Ry.

the alkali metals, the phase shifts, and hence the discontinuities of derivative, are generally small, and this process is rapidly convergent. For the less free electron, like that of the alkali metals, the phase shifts are larger and convergence is slower. But for these metals the experimental data are very much less accurate, and adequate convergence is obtained without increasing the size of the secular determinant.

We consider next the approximation involved in truncating the series of phase shifts. In most of the calculations reported here the s , p , and d phase shifts were treated as adjustable parameters, and the higher phase shifts were set equal to zero. We have shown that for sodium the f phase shift is probably extremely small, and that only for potassium are the experimental data sufficiently accurate to show the influence of the f phase shift. If we may assume that the f phase shift in potassium is positive, and lies between 0 and 0.0005 rad,²⁶ then the corresponding uncertainty in the s , p , and d phase shifts (which must be readjusted to restore the Friedel sum to the value appropriate to E_F as in Table VIII), is about twice as great as that

TABLE VII. Illustrating the sensitivity of the shape of the computed Fermi surface to the size of the secular determinant.^a

n	$10^4(k_{100} - k_{111})/k_0$	$10^4(k_{110} - k_{111})/k_0$
30	25.48	25.06
40	25.41	25.06
50	25.52	25.11
60	25.49	25.08

^a Radial distortions of the Fermi surface of potassium with $\eta_0 = -0.1381$, $\eta_1 = -0.0109$, $\eta_2 = +0.0233$, and $E_F = 0.16$ Ry. The size of the secular determinant is $n \times n$. Corrections for uniform contraction of surface of constant energy when n is increased from 30 to 60:

$$\delta\eta_0 = -0.00013, \quad \delta\eta_1 = -0.00003, \quad \delta\eta_2 = -0.00001.$$

²⁶ The estimate $\eta_3 \approx +0.0005$ rad in potassium was taken from unpublished calculations by J. F. Kenney (private communication).

TABLE VIII. Sets of phase shifts corresponding to the best fit to the Fermi-surface data for potassium, for different values of η_3 .

E_F (Ry)	η_0	η_1	η_2	η_3	$\mathcal{F}(E_F)$
0.13	+0.0412	+0.0532	+0.0252	+0.0005	+0.2104
0.14	-0.0210	+0.0335	+0.0253	+0.0005	+0.1335
0.16	-0.1381	-0.0109	+0.0233	0	-0.0346
0.17	-0.1977	-0.0351	+0.0216	0	-0.1241
0.17	-0.1927	-0.0352	+0.0209	-0.0005	-0.1258
0.18	-0.2521	-0.0608	+0.0184	-0.0005	-0.2205

due to the experimental error. Phase shifts for higher angular momentum decrease rapidly with increasing l and, furthermore, the summation over l in the secular determinant is rapidly convergent. It is unlikely therefore that, even for potassium, our neglect of the phase shifts for $l \geq 4$ introduces any appreciable error into our estimates of the s , p , and d phase shifts.

Finally we consider the approximations involved in carrying out the calculations with a secular determinant derived for a nonlocal potential of muffin-tin form. The muffin-tin potential is an idealization of the true potential in two respects. Firstly, it is assumed that the potential is spherically symmetric within the muffin-tin sphere, and secondly, the potential is taken as constant between the spheres. De Cicco²⁷ has developed methods of correcting for these approximations within the framework of the APW method. It is not possible to express the corrected secular equation explicitly in terms of a set of phase shifts. However, in the course of a calculation of the electronic band structure of potassium chloride, De Cicco found that these corrections were rather small. The excellent agreement of the distortions of our computed Fermi surface for potassium with the experimental data (Fig. 3)²⁸ confirms geometrical arguments which suggest that any small corrections may be absorbed into the phase shifts. That the d and f phase shifts for sodium are very close to zero shows that any corrections are rapidly convergent in l .

In an attempt to estimate the errors involved in truncating the potential at the inscribed sphere, we have computed the best set of phase shifts to fit the potassium data for a series of muffin-tin radii. It will be seen from the results of these calculations in Table IX that the phase shifts are largely independent of the muffin-tin radius over the range of radii we have investigated, and that the small fluctuations of the phase shifts are little greater than the experimental error. For a muffin-tin potential, the Friedel sum of the phase shifts is determined only by the Fermi energy on the APW scale, and the individual phase shifts for a given energy are independent of the muffin-tin radius.

²⁷ P. D. DeCicco, Phys. Rev. **153**, 931 (1967).

²⁸ The experimental points are taken from Ref. 9, and represent the mean of six sets of experimental data in the (100) and (110) zones, respectively. It is thought that the greater accuracy of the fit to the experimental data in the (100) zone reflects the larger amount of experimental data taken in that zone.

Significant dependence of the phase shifts on the muffin-tin radius would indicate substantial departures of the potential from muffin-tin form. Furthermore, it is evident from our results that the secular equation may be solved with a muffin-tin radius greater than the radius of the inscribed sphere, without introducing discontinuous changes in the phase shifts. Thus the phase shifts obtained by analyzing the experimental Fermi surface distortions are found to be largely independent of the radius of the muffin-tin sphere, and they are therefore largely independent of our use of a secular equation based on the muffin-tin approximation.

DISCUSSION

Phase-Shift Method as an Inversion Scheme

We have found that the phase-shift method has several advantages as a technique by which the radial distortions of Fermi surfaces may be computed from the anisotropies of their cross-sectional areas. Perhaps the most important of these is the rapid convergence of the adjustable parameters, the phase shifts η_l . Even for potassium, the distortions of whose Fermi surface are known to high accuracy, an excellent fit to the experimental data is obtained with only four nonzero phase shifts. Our results suggest that significant dependence of the fit to the experimental data on the choice of the Fermi energy parameter E_F may be taken as evidence for incomplete convergence in the series of phase shifts, and that the quality of the fit is largely independent of E_F . However, this conclusion is based on results in which E_F was confined to energies rather close to the free-electron Fermi energy.

A consequence of the small number of fitting parameters involved in the phase-shift method is that only a small amount of experimental data is needed to obtain a rather accurate picture of the Fermi surface. More detailed data help to confirm and to refine the interpretation; however, it appears that the phase-shift method, being derived in a certain approximation from the full many-body theory of electrons in metals, makes the most efficient use of the available experimental data.

Secondly, the Fermi-surface distortions are found to be approximately linear functions of the phase shifts.

TABLE IX. Sensitivity of the best values of the phase shifts to variation in the radius of the muffin-tin sphere. Data for potassium: $E_F = 0.16$ Ry; $\eta_3 = 0$.

R_S (a.u.) ^a	η_0	η_1	η_2	$\mathcal{F}(\eta_l)$
3.675	-0.1416	-0.0106	+0.0242	-0.03331
3.975	-0.1388	-0.0108	+0.0235	-0.03420
4.275	-0.1381	-0.0109	+0.0233	-0.03456
4.575	-0.1408	-0.0106	+0.0236	-0.03473
4.861	-0.1385	-0.0107	+0.0232	-0.03479

^a Inscribed-sphere radius = 4.275 a.u. Wigner-Seitz sphere radius = 4.861 a.u.

This feature of the method is a consequence of the physical significance of the phase shifts, and it simplifies greatly the process of fitting the experimental data.

Finally, the phase-shift method may be applied equally to nearly-free-electron metals and to metals of the transition series. Preliminary phase-shift calculations on the noble metals²⁹ have shown excellent agreement of the computed surfaces with the experimental data. Only in application to that group of semimetals and semiconductors whose crystal structures in the solid state are determined by covalent bonding, and for which a muffin-tin potential is known to be a poor approximation, would we expect the phase-shift method to fail.

Significance of the Phase Shifts

The method of phase-shift analysis applied to Fermi-surface data allows one to investigate the interaction of conduction electrons with the metallic lattice. Solving the secular equation is equivalent to constructing those solutions of a multiple scattering problem in which a disturbance acts on a lattice of ions, generating scattered waves which combine to recreate the original disturbance. The Bloch functions that describe the electronic states of the lattice are such self-consistent disturbances. In the muffin-tin approximation, the wave function in the region of constant potential may be represented as a sum of plane waves. The plane waves are scattered by the muffin-tin cores, generating outgoing spherical waves which may be expressed as a series of partial waves of increasing angular momentum, each partial wave being characterized by an energy-dependent phase shift. At a given energy, the multiple scattering problem is completely defined by the set of partial-wave phase shifts. So also is the set of wave vectors associated with the Bloch functions which are solutions of that problem. The set of wave vectors corresponding to solutions of the multiple scattering problem at the Fermi energy defines the Fermi surface. The distortions of the Fermi surface from the free-electron sphere are therefore completely defined by the set of partial-wave scattering phase shifts appropriate to the Fermi energy. Conversely, the magnitudes of the phase shifts (modulo π) may be deduced from an analysis of the experimental distortions of the Fermi surface from the free-electron sphere.

Certain qualitative features of the variation of the phase shifts within the alkali series may be recognized in the results quoted in Table IV, despite our uncertainty about the correct choice of the Fermi energy parameter E_F . Let us consider first the d phase shifts. For lithium, sodium, and potassium there are no d -like core states and we expect the d phase shifts to be small and, if they are derived from a simple potential, positive. For these metals, the reduced phase shifts are equal to the true phase shifts for scattering by the

ionic potential. It will be seen (Table IV) that over most of the energy range the d phase shift for lithium does not differ significantly from zero. Our results suggest that the Fermi energy on the APW scale may be depressed somewhat with respect to the free-electron value. A similar conclusion follows from the experimental value of the d phase shift in sodium; again the phase shift is very close to zero, and the fact that it is slightly negative over most of the energy range may indicate that the Fermi energy is depressed with respect to the free-electron value, or it may result from small negative many body and other corrections which have been folded into the phase shifts as a consequence of our method of analysis. The d phase shifts in potassium, rubidium, and cesium are positive and perhaps an order of magnitude larger than in lithium and sodium. The large positive d phase shifts mark the onset of d resonances and are related to the position of these alkali metals at the heads of the $3d$, $4d$, and $5d$ transition series. These large d phase shifts show that the shapes of the Fermi surfaces of potassium, rubidium, and cesium are strongly influenced by the d bands above the Fermi surface, confirming and generalizing the conclusion of Lee and Falicov.⁹

The p phase shift of lithium is large and positive over a rather extended energy range. Since there are no p -like core states in lithium, the reduced phase shifts are equal to the true phase shifts, and it will be seen that the shape of the Fermi surface of lithium is strongly influenced by the onset of the p resonance which corresponds to the creation of p -like bound states along the second row of the periodic table. The heavier alkali metals all have p -like core states, and the reduced phase shifts may be positive or negative, so the results admit of no immediate interpretation.

Since all the alkali metals have s -like core states, the reduced phase shifts may be positive or negative and again our results allow no simple interpretation.

Thus the reduced phase shifts derived from the experimental shapes of the Fermi surfaces of the alkali metals are consistent with the results of simple qualitative arguments based on the expected resonance behavior of the phase shifts. Conversely, the distortions of the Fermi surfaces of the alkali metals from a free-electron sphere are systematically influenced by the position of each metal in the periodic table.

The most direct indication of the difference between the phase shifts deduced in the present work and those appropriate to the neutral pseudoatoms of Ziman,³⁰ is gained by comparing the corresponding values of the Friedel sum. For phase shifts derived from the Fermi surface data we have no *a priori* knowledge of the value of the Friedel sum. It is probably close to zero, and its sign may be positive or negative depending on whether there is a small net displacement of conduction charge into or out of the muffin-tin sphere in the metal,

²⁹ M. J. G. Lee (to be published).

³⁰ J. Ziman, *Advan. Phys.* **13**, 89 (1964).

relative to a uniform charge distribution. However, the phase shifts corresponding to the neutral pseudoatoms derived from the monovalent metals satisfy

$$\mathfrak{F}(\eta_i) = 1$$

since the neutral pseudoatom is defined as an ion together with its full screening charge, so that on average one electronic charge must be displaced by the potential into the muffin-tin sphere around each ion.

Equation (15) suggests that our model would reduce to the neutral pseudoatom model of the metal if we were to attempt to fit the Fermi-surface data with $E_F = 0$. The charge density outside the spheres would then fall to zero, corresponding to a Friedel sum of unity. However, the charge distribution would not approximate well the charge distribution in the real metal, and it seems unlikely that the Fermi-surface data would give useful information about the pseudoatom phase shifts. We have not investigated the behavior of the phase shifts in this limit.

Influence of Many-Body Effects

We have shown above [Eqs. (1)–(10)] that in the approximation where lifetime effects may be neglected, the many body theory of conduction electrons in metals leads to a dispersion relation which may be derived from a single-particle-like Schrödinger equation in which the many-body effects are absorbed into an energy and momentum-dependent effective potential. This result explains our success in fitting the experimental Fermi-surface data on potassium with a secular determinant based on the one-electron approximation.

By adjusting the phase shifts to fit the experimental data, we have absorbed the many-body corrections into the phase shifts. Thus it is the effective potential implied by our results, rather than the experimental distortions of the Fermi surface, that we should examine for evidence of many-body effects. Since we have reason to believe that the experimental phase shifts must be derived from an angular-momentum-dependent effective potential, it is not possible to deduce the form of the effective potential directly from our results. We therefore regard our results as imposing a condition on the effective potential, whose form must be proposed on other grounds.

Slater,³¹ and Kohn and Sham,³² have proposed approximate techniques by which exchange and correlation effects in the solid state may be included in an effective potential. These two approximations lead to quite different predictions of the Fermi energy on the APW scale (Table II), and of the phase shifts at the Fermi energy.³³ Our results provide in convenient form a criterion which must be satisfied by the phase shifts

associated with any acceptable effective potential of muffin-tin form. At some energy (the Fermi energy) the phase shifts deduced from the proposed effective potential must agree with the phase shifts derived from the experimental data. Only if this condition is satisfied can the proposed effective potential lead to an accurate prediction of the shape of the Fermi surface.

Kuhn and Van Vleck,³⁴ Brooks and Ham,³⁵ and Heine and Abarenkov,⁶ in theoretical discussions of the electronic structures of the alkali metals, have avoided the problem of representing exchange and correlation effects by an effective potential, by extrapolating from the atomic spectra various parameters related to the scattering phase shifts. Our results provide a criterion by which the success of these methods also might be judged.

Influence of Relativistic Effects

We have not explicitly taken account of relativistic effects in the course of the present work. Yet relativistic effects are known to play a significant role in determining the band structures, and hence the shapes of the Fermi surfaces, of the heavier metallic elements. Such effects might most naturally be taken into account by solving the Dirac equation for a potential of muffin-tin form. The relativistic generalization of the APW method has been discussed by Loucks³⁶ and by Koelling.³⁷

Three new terms are introduced into the one-electron Hamiltonian; these represent the relativistic mass-velocity and Darwin corrections, and the spin-orbit interaction. Since the first two terms are radial functions, they may be treated as corrections to the crystal potential within the muffin-tin sphere. The resulting secular determinant is identical with that of Eqs. (9) and (10), except that the logarithmic derivatives of the radial wave function at the surface of the muffin-tin sphere are replaced by somewhat more complicated parameters.³⁷ The third relativistic correction, the spin-orbit interaction, mixes spinor components and results in a further term in the secular determinant which cannot be expressed analytically as a correction to the phase shifts.³⁷

In the present work we have fitted the experimental Fermi surface data by adjusting the phase shifts, or equivalently the logarithmic derivatives of the non-relativistic radial wave function, which are related to the phase shifts by Eq. (12). In the presence of significant mass-velocity and Darwin terms, which represent the dominant relativistic corrections in the free alkali atoms,³⁸ this procedure is still appropriate, al-

³⁴ T. S. Kuhn and J. H. Van Vleck, *Phys. Rev.* **79**, 382 (1950).

³⁵ H. Brooks and F. S. Ham, *Phys. Rev.* **112**, 344 (1958).

³⁶ T. L. Loucks, *Phys. Rev.* **139**, 231 (1965).

³⁷ D. Koelling, Quarterly Progress Report No. 68, Solid State and Molecular Theory Group, Massachusetts Institute of Technology, 1968 (unpublished).

³⁸ F. Herman and S. Skillman, *Atomic Structure Calculations* (Prentice-Hall, Inc., Englewood Cliffs, N. J., 1963).

³¹ J. C. Slater, *Phys. Rev.* **81**, 385 (1951).

³² W. Kohn and L. J. Sham, *Phys. Rev.* **140**, 1133 (1965).

³³ J. F. Kenney (private communication).

though the relativistic corrections modify somewhat the significance of the phase shifts. Thus, within the limits of validity of the relativistic APW method the mass-velocity and Darwin corrections may be folded into the phase shifts.

In general, the spin-orbit term may cause the splitting of accidental degeneracies and orbital degeneracies, thereby modifying the form of the energy bands near such degeneracies. However, there are no accidental degeneracies close to the Fermi energy in the band structure of cesium.³⁹ The nonrelativistic energy bands suggest that the most significant effect of spin-orbit interaction on the Fermi surface of cesium would be a distortion of the surface along the $\langle 111 \rangle$ direction, resulting from a splitting of the orbital degeneracy of the lowest p -like state P_4 . If we may assume that the splitting of the energy bands at P is of the same order of magnitude as the spin-orbit splitting of the $6p$ states in atomic cesium, and that the one-electron states are predominantly p -like on the Fermi surface in the $\langle 111 \rangle$ direction, then a simple perturbation argument shows that the energy band along Λ would be depressed by energy δE , given by

$$(\delta E/E_F) \approx - (V_{so}^2/E_{gap}E_F),$$

where V_{so} is the spin-orbit splitting at P , E_{gap} is the energy gap between the unperturbed state on the Fermi surface along $\langle 111 \rangle$ and the next highest band at the same point in the Brillouin zone, and E_F is the free-electron Fermi energy. Taking $V_{so} \approx 0.005$ Ry,⁴⁰ $E_{gap} \approx 0.08$ Ry,³⁹ and $E_F \approx 0.12$ Ry (Table II), we find

$$(\delta E/E_F) \approx -2.6 \times 10^{-3}.$$

This result suggests that the spin-orbit interaction may contribute to only a rather small extent to the radial distortion of the Fermi surface. To a first approximation the radial distortion may be estimated from the free-electron dispersion relation

$$(\delta k/k) \approx -(\delta E/2E_F) \approx +1.3 \times 10^{-3} \text{ along } \langle 111 \rangle,$$

and the result suggests that the spin-orbit interaction may contribute less than 5% of the experimentally observed distortion of the Fermi surface.

In the lighter alkali metals the Fermi surfaces are substantially less distorted than is that of cesium, but the increased sensitivity of the Fermi surface to spin-orbit effects is more than offset by the rapid decrease of the magnitude of the spin-orbit splitting. For these reasons we believe that neglect of the spin-orbit interaction is a valid approximation in our discussion of the shapes of the Fermi surfaces of the alkali metals.

³⁹ J. F. Kenney, Quarterly Progress Report No. 66, Solid State and Molecular Theory Group, Massachusetts Institute of Technology, 1967 (unpublished).

⁴⁰ C. E. Moore, *Atomic Energy Levels* (National Bureau of Standards, Washington, D. C., 1949).

CONCLUSIONS

We have shown how the partial-wave phase shifts which describe the interaction between the conduction electrons and the ion cores in a metallic lattice may be derived from experimental Fermi-surface data. An analysis of the experimental distortions of the Fermi surfaces of the alkali metals indicates that the shapes of the Fermi surfaces are systematically influenced by the position of each metal in the periodic table.

We have found that, for sodium and potassium, the best values of the three phase shifts η_0 , η_1 , and η_2 lead to surfaces of constant energy whose area distortions are in excellent agreement with the experimental Fermi-surface data. We have applied the phase-shift method to estimate the radial distortions of the Fermi surfaces of all the alkali metals, and have suggested that the radii computed in this way may be substantially more accurate than earlier results. Experience with calculations based on muffin-tin potentials suggests that the present method may be applied successfully to the analysis of experimental Fermi-surface data on a large group of metals, including nearly-free-electron metals and transition metals, and excluding only that group of semimetals and degenerate semiconductors in which directional bonding is known to be important.

Finally, we have pointed out that our experimental phase shifts include corrections for exchange and correlation effects, as well as for certain relativistic effects. Thus, the phase shifts derived from any effective potential of muffin-tin form that may be proposed to take into account exchange and correlation effects for conduction electrons in the alkali metals, must be consistent with the present results.

ACKNOWLEDGMENTS

I have benefited from many helpful and stimulating discussions in the course of the present research. In particular, I am indebted to Professor T. L. Loucks and to Dr. F. M. Mueller for discussions about the APW method, and to Professor M. H. Cohen for discussions about some aspects of many-body theory. My thanks are due to Dr. J. F. Kenney for allowing me to use results from his unpublished band-structure calculations, and to Dr. L. F. Mattheiss and E. I. Zornberg for giving me copies of several digital computer programs. Finally, I wish to express my gratitude to Dr. D. Shoenberg, who introduced me to the experimental study of the Fermi surfaces of the alkali metals. This research was greatly facilitated by the excellent service given by the Computation Center of the University of Chicago. This research was supported in part by the National Aeronautics and Space Administration, and also benefited from the use of facilities provided by the Advanced Research Projects Agency for materials research at the University of Chicago.